Online Resources to the paper Hess et al. (2020) "*PioLaG: A piosphere landscape generator for savanna rangeland modelling*", Landscape Ecology

Online Resource 1

Piosphere patterns in classified aerial images

1. Classification of aerial images

To be able to classify the simulated model results and verify the approximation to the real world, we compared PioLaG outputs with piosphere patterns quantified on aerial images of real savanna landscapes. The aerial images were provided by the National Geo-Spatial Information (NGI) South Africa, covering the whole Molopo region. The images were taken during the dry season in July 2013 and have a resolution of 0.5 m which allowed for the visual detection of 10 obvious animal concentration points (watering points, kraals). These points served as the center for a 3 x 3 km aerial image tile. For these tiles, the Visible Vegetation Index [*VVI*, Eq. 1; (PHL 2015)] was calculated from the available RGB bands to enhance vegetation characteristics.

$$VVI = \left[\left(1 - \left|\frac{red - 30}{red + 30}\right|\right)\left(1 - \left|\frac{green - 50}{green + 50}\right|\right)\left(1 - \left|\frac{blue - 1}{blue + 1}\right|\right)\right] \quad (1)$$

Land cover classes were then determined in an unsupervised classification approach. A k-means algorithm, implemented in R (R Core Team 2018) was applied to cluster each of the tiles based on their RGB bands and VVI. The number of classes was determined by the comparison of the sum of squares within the separate cluster to the total sum of squares for different amounts of clusters. The identified optimal number of clusters was four. Hence, the images were clustered into four classes, which were then assigned to the corresponding land cover class on the basis of the *VVI*. The visual interpretation and comparison with the aerial image let to the interpretation of these four classes as *bare ground* (low *VVI*), *herbaceous vegetation* (two classes, medium *VVI*) and *woody vegetation* (high *VVI*). However, due to the constraints of limited image bands (RGB) and the difficult spatial patterning of vegetation (no larger connected patches but rather inter-mixed and clustered vegetation with no clear boundaries) providing no indication for a reasonable distinction of herbaceous vegetation types, we decided to combine the two corresponding classes.

2. Site selection and calculation of piosphere patterns

We identified a total of 31 watering points [or similar structures with clear signs of regular animal concentration and radial vegetation patterns (piospheres)] in the portion of the Molopo region for which we had aerial-image coverage. This selection was carried out visually with the aid of RGB satellite images in QGIS (version 2.18.9; with the open layers plugin: google satellite). The vegetation patterns and corresponding distribution of land-cover classes were quantified on the classified aerial images (see above) using R version 3.4.4 (R Core Team 2018). First, we created 10-m buffer donuts up to 1000 m around each watering point and determined the relative frequency of the dominant vegetation types (land cover classes) for each distance donut. The distance of 1000 m corresponded to local camp sizes as measured on the images. In a second step, we plotted the mean frequency of the three different vegetation types against the distance from the watering point (herbivore-use intensity gradient) in reference (1) to all 31 watering points (piospheres) and (2) to three configurations of vegetation differing in the proportion of woody vegetation (trees and shrubs). Chosen thresholds for woody vegetation within the 1000-m buffer zone were: low ($\leq$ 17% woody vegetation; n = 15), medium (> 17% and $\leq$ 25% woody vegetation; n = 11) and high (> 20%; n = 5). Contrary to grasses and forbs, the abundance pattern of established woody vegetation is relatively stable over time, at least in the short- to medium term. It also determines the competitive environment for the herbaceous layer. Hence, the additional distinction of savanna vegetation configurations allowed us to contrast different real-world scenarios that not only represent snapshots in time.

3. Results of classified aerial image analysis

Piospheres with an overall low proportion of woody vegetation (Fig. OR1.1A) were characterized by much bare soil along the whole 1000-m gradient from the watering point. However, there was clear indication of a sacrifice zone with a steadily increasing proportion of herbaceous vegetation, which leveled-off at about 38% at a distance of 250 m. In piospheres with a medium proportion of woody vegetation (Fig. OR1.1B), herbaceous vegetation became already dominant after 130 m from the watering point and bare soil dropped below 38%. In contrast, piospheres with a relatively high proportion of woody vegetation (Fig. OR1.1C) displayed the shortest sacrifice zone with an almost abrupt drop of bare soil within the first 100 meters to values between 10% and 20% and a sharp increase of herbaceous vegetation to nearly 50%. These proportions remained quite constant along the gradients. Averaged over all 31 piospheres (Fig. OR1.1D), the basic vegetation pattern described a moderate increase of herbaceous vegetation at the expense of bare ground with no indication of a zone of denser woody vegetation along the gradients.

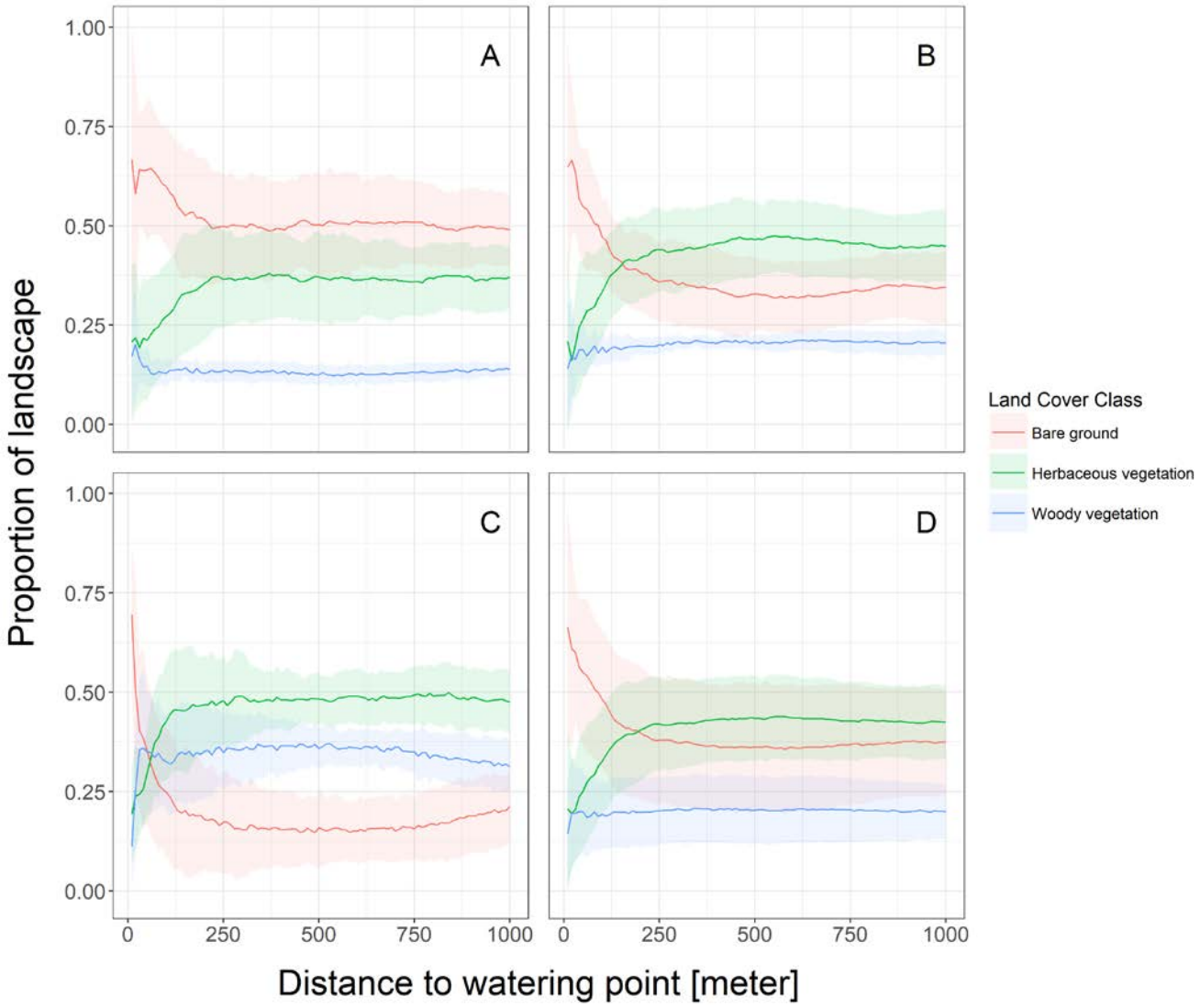

Fig. OR1.1 Distribution of land cover classes around watering points identified on aerial images of the Molopo savanna in South Africa. A total of 31 piospheres were subdivided into vegetation configurations with (A) low (≤ 17%, n = 15), (B) medium (>17% and ≤ 25%, n = 11) and (C) high (> 25%, n = 5) proportions of woody vegetation (trees and shrubs) as a relatively constant variable. (D) Piosphere plot with the proportional vegetation types averaged over all 31 watering points.

4. Similarities between aerial images and generated landscapes

The piospheres recreated with the piosphere landscape generator (PioLaG) were much more complex but their basic vegetation patterns were comparable to the patterns quantified on the aerial images. Similarities include the sacrifice zone of varying width and dominated by bare soil in close vicinity to the watering point, as well as the constant increase of herbaceous vegetation thereafter. This is especially true when combining the response of annual-, palatable perennial- and unpalatable perennial grasses in PioLaG, which

could not be differentiated on the aerial images. However, in the simulated landscape, all scenarios included a rather humped-shaped distribution of cells dominated by woody vegetation, while in the aerial images the proportion of woody vegetation remained relatively stable along the whole gradient beyond the sacrifice zone. This is in sharp contrast to savanna piosphere patterns described in scientific literature (compare main text). However, as bush thickening is widespread in the Molopo area (and consequently corresponding patterns also visible on aerial images), the rather open savannas detected could result from active interventions like bush control, which is commonly conducted in the area to restore a productive grass layer (Harmse et al. 2016). In this respect, our identification of 31 piospheres may also be biased towards clearly visible watering points, because such located in denser stands of woody vegetation are more likely overlooked. Another problem with the aerial images is that they are not representative for the full potential of vegetation. Accordingly, insufficient and patchy rainfall, a fire event or high grazing pressure preceding the date of the images may have accounted for the observed relatively high proportion of bare ground also beyond the sacrifice zones, a pattern not displayed by PioLaG as well (at least under the chosen simulation settings). It is therefore that for additional verification of the PioLaG piospheres in reference to real-world scenarios, further site-specific assessments and analyses would be necessary that allow to consider the local management history (e.g. with respect to stocking rates, resting periods or bush control measures) and other disturbances (e.g. fire events, rainfall patterns or drought periods).

References

Harmse CJ, Kellner K, Dreber N (2016) Restoring productive rangelands: A comparative assessment of selective and non-selective chemical bush control in a semi-arid Kalahari savanna. J Arid Environ 135:39–49. doi: 10.1016/j.jaridenv.2016.08.009

PHL (2015) Visible Vegetation Index (VVI) - Technical Report. University of Puerto Rico at Arecibo. http://phl.upr.edu/projects/visible-vegetation-index-vvi

R Core Team (2018) R: A Language and Environment for Statistical Computing

Online Resource 2

Input data used for PioLaG

Table OR2.1 Classification of stocking situation on farm and associated parameters

Stocking rate class	**Stocking ratio**	**Stocking factor (Parameter that affects slope of HUI curve)**
Under-stocked	($x < 0.9$)	1.5
Optimally-stocked	($0.9 < x \leq 1.0$)	1
Over-stocked	($1.0 < x \leq 1.5$)	0.9
Severely over-stocked	($1.5 < x$)	0.8

Table OR2.2 Classification of clay percentage and associated parameter values

Clay percentage class	**Clay percentage**	**Parameter** *(soilBushFactor)*
Low	($x < 30\%$)	0.8
Medium	($30\% \leq x < 50\%$)	0.7
High	($x \geq 50\%$)	0.6

Table OR2.3: Classification of severity of bush thickening in outer piosphere and associated parameter values

Severity of bush thickening	**Parameter** *(severityOfBushEncroachment)*
Low	0.33
Medium	0.5
High	1

Online Resource 3

Example of two common types of spatial camp arrangements in the Molopo region of South Africa

The examples clearly show straight fence lines with a central watering point (or similar animal concentration point). Tracks along the fences and the area directly surrounding the watering points appear bright as a result of dominant bare soil.

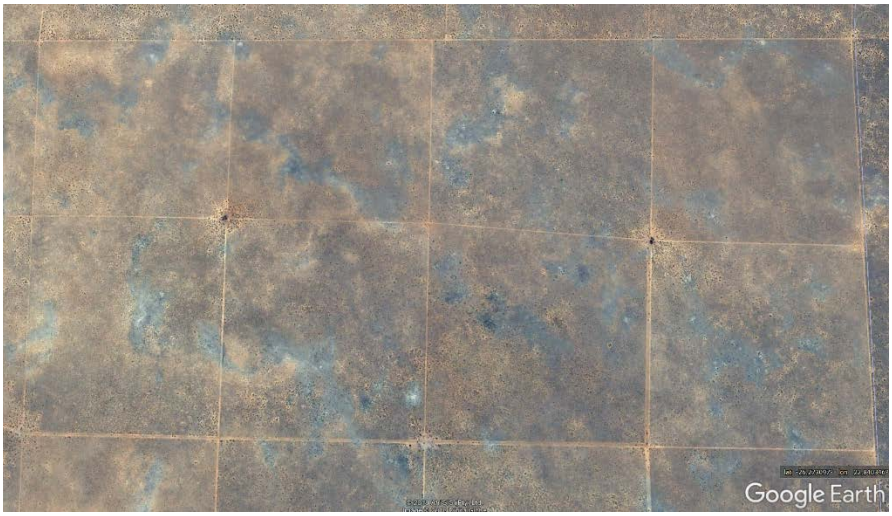

Fig. OR3.1 Square camp arrangement (26°16'16.2"S 22°50'21.6"E; google earth)

Fig. OR3.2 Wagon wheel shaped camp arrangement (25°41'31.54812"S 23°20'26.69604"E; google maps)

Online Resource 4

Additional generated landscape scenarios

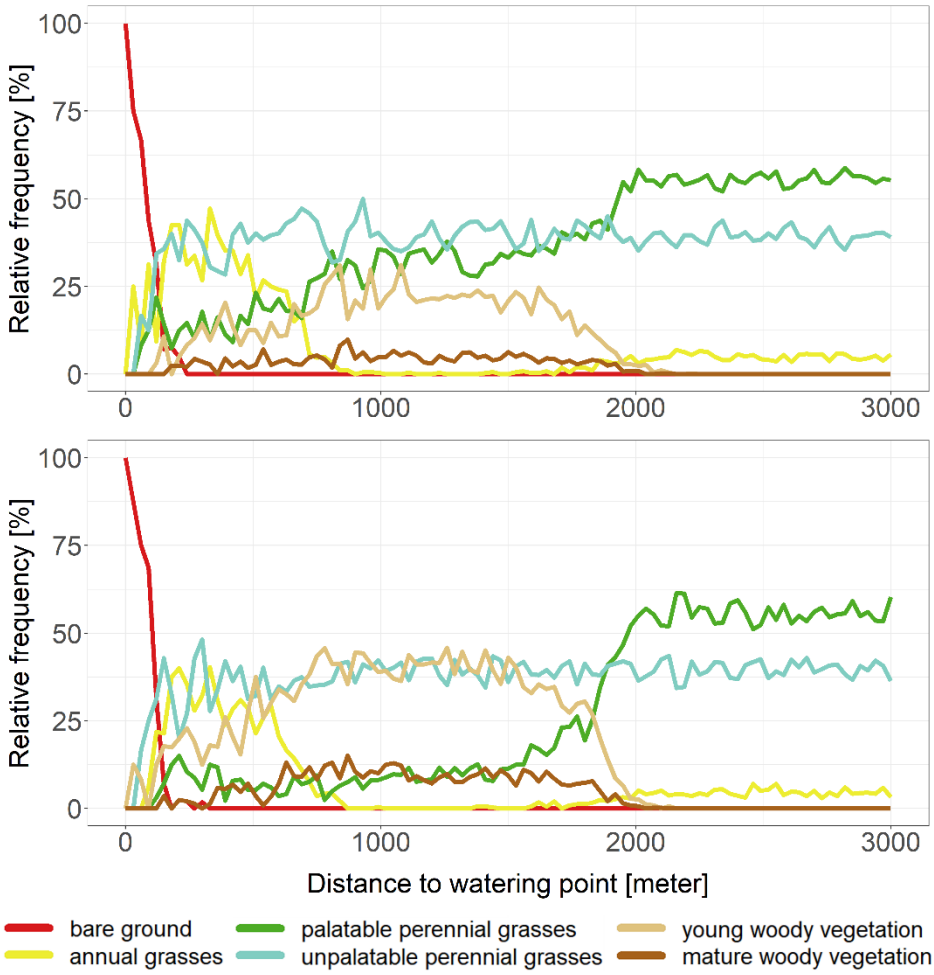

Fig. OR4.1 Piosphere graphs of a scenario with low mean annual precipitation (124mm) and low clay content (5%) in the soil (top) and with high mean annual precipitation (490mm) and a high clay content (27%) in the soil (bottom).

Table OR4.1 Model parameterization in Figure OR4.1/top.

Longitude (x)	23	**bush-thickened camps**	0
Latitude (y)	-26	**severity of thickening**	NA
MAP	124 mm	**rotational grazing**	On
Farm size	14400 ha	**auto-setup-mode**	On
stocking rate	13 ha/LSU	**camp layout**	rectangular
grazing capacity	12 ha/LSU	**camp layout**	2 cols; 2 rows
stocking ratio	0.92 = optimally stocked	**no. of watering points**	1
		clay content	0.05

Table OR4.2 Model parameterization in Figure OR4.1/bottom.

Longitude (x)	23	**bush-thickened camps**	0
Latitude (y)	-26	**severity of thickening**	NA
MAP	490 mm	**rotational grazing**	On
Farm size	14400 ha	**auto-setup-mode**	On
stocking rate	13 ha/LSU	**camp layout**	rectangular
grazing capacity	12 ha/LSU	**camp layout**	2 cols; 2 rows
stocking ratio	0.92 = optimally stocked	**no of watering points**	1
		clay content	0.27

Online Resource 5

Parameterization (parameter settings) for the analyzed scenarios in Figures 4 to 8 (main text)

Table OR5.1 Model parameterization in Figure 4.

Longitude (x)	23	**bush-thickened camps**	0
Latitude (y)	-26	**severity of thickening**	NA
MAP	405 mm	**rotational grazing**	On
Farm size	14400 ha	**auto-setup-mode**	On
stocking rate	13 ha/LSU	**camp layout**	rectangular
grazing capacity	12 ha/LSU	**camp layout**	2 cols; 2 rows
stocking ratio	0.92 = optimally stocked	**no. of watering points**	1
		clay content	0.03

Table OR5.2 Model parameterization in Figure 5a.

Longitude (x)	23	**bush-thickened camps**	0
Latitude (y)	-26	**severity of thickening**	NA
MAP	405 mm	**rotational grazing**	On
Farm size	14400 ha	**auto-setup-mode**	On
stocking rate	20 ha/LSU	**camp layout**	rectangular
grazing capacity	12 ha/LSU	**camp layout**	2 cols; 2 rows
stocking ratio	0.6 = understocked	**no. of watering points**	1
		clay content	0.03

Table OR5.3 Model parameterization in Figure 5b.

Longitude (x)	23	**bush-thickened camps**	0
Latitude (y)	-26	**severity of thickening**	NA
MAP	405 mm	**rotational grazing**	On
Farm size	14400 ha	**auto-setup-mode**	On
stocking rate	13 ha/LSU	**camp layout**	rectangular
grazing capacity	12 ha/LSU	**camp layout**	2 cols; 2 rows
stocking ratio	0.92 = optimally stocked	**no. of watering points**	1
		clay content	0.03

Table OR5.4 Model parameterization in Figure 5c.

Longitude (x)	23	**bush-thickened camps**	0
Latitude (y)	-26	**severity of thickening**	NA
MAP	405 mm	**rotational grazing**	On
Farm size	14400 ha	**auto-setup-mode**	On
stocking rate	6 ha/LSU	**camp layout**	rectangular
grazing capacity	12 ha/LSU	**camp layout**	2 cols; 2 rows
stocking ratio	2,0 = severely overstocked	**no. of watering points**	1
		clay content	0.03

Table OR5.5 Model parameterization in Figure 6a.

Longitude (x)	28.64	**bush-thickened camps**	0
Latitude (y)	-25.05	**severity of thickening**	NA
MAP	490 mm	**rotational grazing**	On
Farm size	14400 ha	**auto-setup-mode**	On
stocking rate	13 ha/LSU	**camp layout**	rectangular
grazing capacity	12 ha/LSU	**camp layout**	2 cols; 2 rows
stocking ratio	0.92 = optimally stocked	**no. of watering points**	1
		clay content	0.05

Table OR5.6 Model parameterization in Figure 6b.

Longitude (x)	21	**bush-thickened camps**	0
Latitude (y)	-30	**severity of thickening**	NA
MAP	124 mm	**rotational grazing**	On
Farm size	14400 ha	**auto-setup-mode**	On
stocking rate	13 ha/LSU	**camp layout**	rectangular
grazing capacity	12 ha/LSU	**camp layout**	2 cols; 2 rows
stocking ratio	0.92 = optimally stocked	**no. of watering points**	1
		clay content	0.27

Table OR5.7 Model parameterization in Figure 7.

Longitude (x)	23	**bush-thickened camps**	0
Latitude (y)	-26	**severity of thickening**	NA
MAP	405 mm	**rotational grazing**	OFF
Farm size	14400 ha		
stocking rate	6 ha/LSU	**camp layout**	rectangular
grazing capacity	12 ha/LSU	**camp layout**	1 cols; 1 rows
stocking ratio	2 =severely overstocked	**no. of watering points**	1
		clay content	0.03

Table OR5.8 Model parameterization in Figure 8.

Longitude (x)	23	**bush-thickened camps**	6
Latitude (y)	-26	**severity of thickening**	high
MAP	405 mm	**rotational grazing**	On
Farm size	14400 ha	**auto-setup-mode**	Off
stocking rate	13 ha/LSU	**camp layout**	rectangular
grazing capacity	12 ha/LSU	**camp layout**	4 cols; 4 rows
stocking ratio	0.92 = optimally stocked	**no of watering points**	4
		clay content	0.03